

Presynaptic Type III Neuregulin 1 Is Required for Sustained Enhancement of Hippocampal Transmission by Nicotine and for Axonal Targeting of $\alpha 7$ Nicotinic Acetylcholine Receptors

Chongbo Zhong,¹ Chuang Du,¹ Melissa Hancock,² Marjolijn Mertz,^{1,4} David A. Talmage,³ and Lorna W. Role^{1,2}

¹Department of Neurosciences and ²Integrated Program in Cellular, Molecular, and Biophysical Studies, Columbia University, New York, New York 10032,

³Department of Pharmacology and Center for Brain and Spinal Cord Research, Stony Brook University, Stony Brook, New York 11794, and ⁴Department of Experimental Neurophysiology, Vrije Universiteit, 1081 HV Amsterdam, The Netherlands

Both the neuregulin 1 (*Nrg1*) and $\alpha 7$ nicotinic acetylcholine receptor ($\alpha 7^*nAChRs$) genes have been linked to schizophrenia and associated sensory–motor gating deficits. The prominence of nicotine addiction in schizophrenic patients is reflected in the normalization of gating deficits by nicotine self-administration. To assess the role of presynaptic type III *Nrg1* at hippocampal–accumbens synapses, an important relay in sensory–motor gating, we developed a specialized preparation of chimeric circuits *in vitro*. Synaptic relays from *Nrg1*^{tm1Lw} heterozygote ventral hippocampal slices to wild-type (WT) nucleus accumbens neurons (1) lack a sustained, $\alpha 7^*nAChR$ -mediated phase of synaptic potentiation seen in comparable WT/WT circuits and (2) are deficient in targeting $\alpha 7^*nAChRs$ to presynaptic sites. Thus, selective alteration of the level of presynaptic type III *Nrg1* dramatically affects the modulation of glutamatergic transmission at ventral hippocampal to nucleus accumbens synapses.

Key words: neuregulin 1; $\alpha 7$ nicotinic acetylcholine receptor; sensory–motor gating; ventral hippocampal–nucleus accumbens synapses; schizophrenia; synaptic plasticity

Introduction

Neuregulin 1 (*Nrg1*)–ErbB signaling regulates synapse formation, synaptic plasticity, and the maintenance of synaptic connections, in part by regulating the levels of functional neurotransmitter receptors (Yang et al., 1998; Huang et al., 2000; Wolpowitz et al., 2000; Liu et al., 2001; Kawai et al., 2002; Falls, 2003; Okada and Corfas, 2004; Gu et al., 2005; Kwon et al., 2005; Chang and Fischbach, 2006; Bjarnadottir et al., 2007; Li et al., 2007). The implication of *Nrg1* as a schizophrenia susceptibility gene underscores the importance of understanding the relationship between *Nrg1* signaling and circuits affected in schizophrenia (Stefansson et al., 2004; Harrison and Weinberger, 2005).

The majority of patients with schizophrenia are heavy smokers, consistent with proposed roles of nicotine as a form of self-medication (Batel, 2000; Kumari and Postma, 2005; Strand and

Nyback, 2005). *Nrg1*–ErbB signaling has been implicated in the regulation of neuronal nicotinic acetylcholine receptors (*nAChR*), in particular the $\alpha 7^*nAChRs$ (Yang et al., 1998; Liu et al., 2001; Kawai et al., 2002; Chang and Fischbach, 2006; Mathew et al., 2007; Hancock et al., 2008), renowned for their role in nicotine-induced plasticity of corticolimbic and mesolimbic circuits (McGehee et al., 1995; Dajas-Bailador and Wonnacott, 2004; Jo et al., 2005; Mansvelder et al., 2006; Couey et al., 2007). Because genetic studies have linked both the *Nrg1* and $\alpha 7$ subunit genes to major endophenotypes of schizophrenia (Leonard et al., 1998; Harrison and Weinberger, 2005; Mathew et al., 2007), we tested whether reduced expression of type III *Nrg1* alters nicotine responsiveness in the ventral striatum, specifically in the nucleus accumbens shell (*nAcc*), in which convergent inputs from prefrontal cortex, ventral hippocampus/subiculum (*vHipp*), ventral tegmental area, and amygdala are integrated to produce context-informed volitional behaviors (Lisman and Grace, 2005; Ronesi and Lovinger, 2005). We demonstrate that presynaptic type III *Nrg1* determines normal levels of presynaptic targeting of $\alpha 7^*nAChRs$ along axons of ventral hippocampal neurons.

Materials and Methods

Genotype-specific *vHipp*–*nAcc* synaptic cocultures. Animals were treated in accordance with the National Institutes of Health *Guide for the Care and Use of Laboratory Animals*. The region of ventral CA1 and subiculum of hippocampi from single wild-type (WT) animals or animals heterozygous for an isoform-specific disruption of type III *Nrg1* (*Nrg1*^{tm1Lw} +/–) (Wolpowitz et al., 2000) were sliced into 150 × 150 μ m pieces and plated in minimal volume of culture media (50 μ l). Dispersed WT *nAcc* neu-

Received Jan. 28, 2008; revised June 30, 2008; accepted July 1, 2008.

This work was funded by Grants NS29071 and DA019941 from National Alliance for Research on Schizophrenia and Depression (Sidney Baer Distinguished Investigator Award to L.W.R.) and the McKnight Foundation (L.W.R.). M.H. was supported by National Institutes of Health Grant T32 DK07328. We thank Drs. S. Siegelbaum, Y. H. Jo, and M. Johnson for suggestions on previous versions of this manuscript.

*C.Z. and C.D. contributed equally to this work.

Correspondence should be addressed to Lorna W. Role at her present address: Department of Neurobiology and Behavior, Stony Brook University, Stony Brook, NY 11794. E-mail: lorna.role@stonybrook.edu.

C. Du's present address: Center for Neuroscience Research, Tufts University School of Medicine, 136 Harrison Avenue, Boston, MA 02111.

C. Zhong's, M. Hancock's, M. Mertz's, and L. W. Role's present address: Department of Neurobiology and Behavior and Center for Brain and Spinal Cord Research, Stony Brook University, Stony Brook, NY 11794.

DOI:10.1523/JNEUROSCI.0381-08.2008

Copyright © 2008 Society for Neuroscience 0270-6474/08/289111-06\$15.00/0

rons (embryonic day 16 to postnatal day 1) were added after the vHipp explants had attached. Additional details of the specialized technique developed for these studies can be found in the legend of Figure 1 and in supplemental data (available at www.jneurosci.org as supplemental material).

Immunostaining and fluorescent visualization. For α -bungarotoxin (α BgTx) labeling, the coverslips were incubated with α BgTx conjugated to Alexa 594 (1:1000; Invitrogen) for 30 min at 37°C before fixation. For standard immunodetection, coverslips were fixed in 4% paraformaldehyde/4% sucrose/PBS (20 min, 4°C), treated with 0.25% Triton X-100/PBS (5 min at room temperature) and 10% preimmune donkey serum in PBS (30 min at room temperature), and then incubated in primary antibody for 2 h and secondary antibody for 1 h at 37°C. Antibodies used included the following: anti-vesicular glutamate transporter 1 (vGluT1) 1:250; Synaptic Systems), anti-GAD65 (1:50; Developmental Studies Hybridoma Bank), and FITC- and rhodamine-conjugated Ig (1:150 to 1:200; Jackson ImmunoResearch). α BgTx clusters (defined as six contiguous pixels at 50% of maximal intensity) were quantified using a custom algorithm with MetaMorph software (version 7.1; Molecular Devices).

Electrophysiological recordings. Macroscopic and synaptic currents were recorded by whole-cell configuration of the patch-clamp technique, with cells held at -60 mV. Preparations were continuously perfused with extracellular solution containing the following (in mM): 145 NaCl, 3 KCl, 2.5 CaCl₂, 10 HEPES, and 10 glucose, pH 7.4. The intracellular solution included the following (in mM): 3 NaCl, 150 KCl, 1 MgCl₂, 1 EGTA, 10 HEPES, 5 MgATP, and 0.3 NaGTP, pH 7.2. Voltage-clamp recordings were performed with a List EPC-7 Patch Clamp Amplifier (Medical Systems). CNQX, AP-5, bicuculline (Tocris Cookson), α BgTx, and TTX (Sigma) were included in the perfusate as noted. (–)–Nicotine (hydrogen tartrate salt) and glutamate were applied via local pressure ejection (Picospritzer; General Valve).

Data collection and statistical analysis. Macroscopic and synaptic currents were filtered at 10 kHz with a eight-pole Bessel filter (direct current amplifier/filter; Warner Instruments) before acquisition and digitization through a DigiData 1200B analog-to-digital interface with pClamp8 (Molecular Devices). Peaks of macroscopic currents were determined by pClamp8 (Fetchan), and decay time constants were calculated with Origin; Microcal Software). Spontaneous synaptic currents, amplitude, rise time, half-decay time, and frequency of miniature EPSCs (mEPSCs) were measured with MiniAnalysis (Synptosoftware). Normally distributed data were assessed for statistical significance by ANOVA with a *post hoc* test for multiple comparisons and group means with unequal sample size. Non-normally distributed data were analyzed using nonparametric methods (Kolmogorov–Smirnov test).

Results

Gene chimeric synapses

We developed a specialized preparation of hippocampal–striatal circuits *in vitro* to study the effects of genetic manipulation of presynaptic neurons in mouse CNS synapses (Fig. 1). vHipp and subicular regions were extirpated from WT or *Nrg1^{tm1Lwr} +/-*

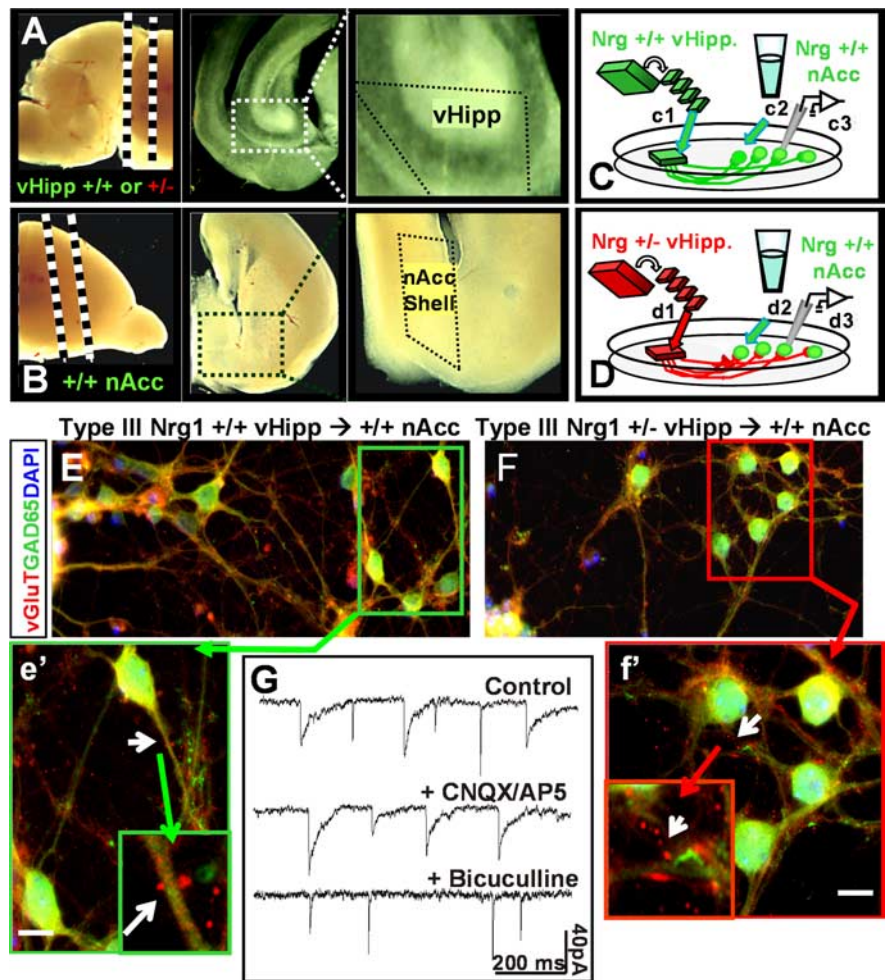


Figure 1. Presynaptic deletion of type III Nrg1 in heterogenotypic corticolimbic circuits *in vitro*. **A**, Microslices of ventral hippocampus/subiculum of WT or *Nrg1^{tm1Lwr} +/-* mice provide glutamatergic projections to dispersed neurons from WT nucleus accumbens (**B**, *+/+* nAcc). **C**, **D**, Genotype-specific circuits are prepared by separate plating of vHipp slices from an individual *+/+* or *+/-* mouse (**C**, c1 and **D**, d1). vHipp microslices of *+/+* or *Nrg1^{tm1Lwr} +/-* mice extend axonal projections (vGluT⁺) that contact nAcc neurons (GAD65⁺; **E**, **e'**, **F**, **f'**). Scale bars, 10 μ m. DAPI, 4',6'-Diamidino-2-phenylindole. vGluT1-positive projections from the vHipp microslices (left) and adjacent sites of vGluT1 (red) and GAD65 (green)-positive staining are indicated (arrows). **G**, Representative recordings from innervated nAcc neurons reveal spontaneous synaptic currents (mPSCs; artificial CSF + TTX; Control). Addition of glutamate receptor blockers (CNQX/AP5) eliminates fast mPSCs, without affecting the slower mPSCs; addition of GABA_A receptor blockers (bicuculline) isolates the glutamatergic synaptic input.

mice (Fig. 1A). Microexplants were plated in minimal volume and allowed to spread [*WT* (Fig. 1C, c1), *+/-* (Fig. 1D, d1)] before the addition of dispersed target neurons from the nucleus accumbens shell (Fig. 1B). We focused our analysis on the role of type III Nrg1 in the presynaptic vHipp projections in regulating plasticity at hippocampal–striatal synapses by keeping the nAcc genotype (WT) constant and varying the genotype of the vHipp slices.

The general features of chimeric *Nrg1^{tm1Lwr} +/-* preparations were indistinguishable from those of sibling cocultures from WT mice. The overall profile of hippocampal glutamatergic fiber outgrowth (vGluT⁺ fibers), the number of vGluT⁺ puncta along vHipp axons, the survival of nAcc neurons (GAD65⁺), and the percentage of nAcc neurons that received synaptic input within 1 week were found to be independent of the presynaptic genotype (Fig. 1E–G).

Patch-clamp recording from contacted WT nAcc neurons after 4–7 d *in vitro* revealed ongoing glutamatergic (microslice-derived) and GABAergic (nAcc to nAcc) synaptic activity,

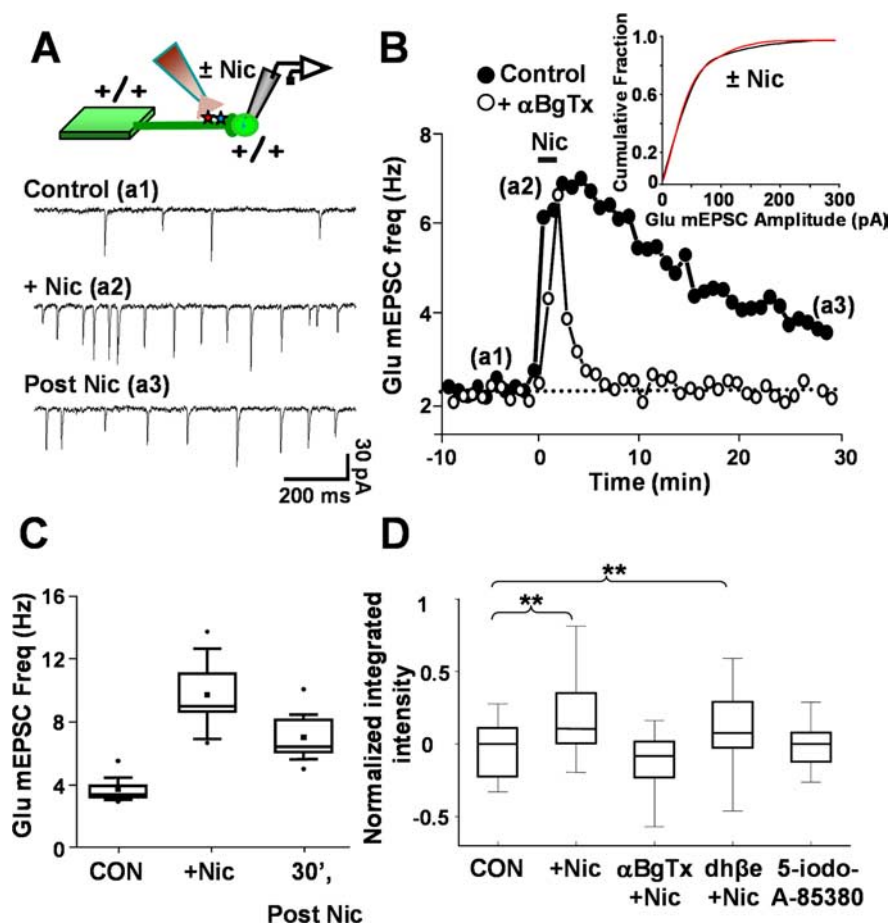


Figure 2. A single application of nicotine elicits a sustained enhancement of transmission at WT vHipp/WT nAcc synapses. **A**, Top, Schematic diagram of the recording configuration used for nicotinic modulation of glutamatergic transmission. **a1**, Control profile of spontaneous glutamate-receptor-mediated synaptic activity (Glu mEPSCs: bicuculline and TTX resistant; CNQX–APV sensitive). **a2**, Spontaneous synaptic currents with nicotine (+Nic) recorded in the same nAcc neuron ~2 min after application and washout of nicotine (500 nM; 1 min). **a3**, Postnicotine records obtained ~30 min after 1 min nicotine application and washout. **B**, Glu mEPSC frequency (in hertz) versus recording time (in minutes). Note that the nicotine-evoked enhancement of mEPSC frequency occurs without change in mEPSC amplitude (inset in **B**: control, black; with nicotine, red, sampled at 5 min before, during, and immediately after **a1** and **a2**). The nicotine-evoked increase includes two pharmacologically, temporally distinguishable phases. The early/acute phase of nicotine-enhanced transmission was resistant to the $\alpha 7^*$ nAChRs-selective antagonist α BgTx (filled circles, \pm Nic at $t = 0$; open circles, + α BgTx). In addition, a sustained enhancement of Glu mEPSCs lasting >30 min after nicotine application was seen at this and at all nicotine-sensitive WT to WT synapses examined (**B**, filled circles; **C**). The sustained component was blocked by α BgTx (**B**, open circles; **C**, **C**). **C**, Box plot of results assaying the time course of nicotine-enhanced transmission at WT to WT synapses. The Glu mEPSC frequency over 2 min of recording under the indicated conditions ($n = 8$ for each condition) is plotted in hertz. A Kolmogorov–Smirnov analysis revealed significant increases in Glu mEPSC frequency in response to a 1 min nicotine application (CON vs Nic, $p < 0.005$) that was still evident 30 min after nicotine addition and washout (CON vs Nic, 30 h, $p < 0.01$). **D**, Box plot analysis evaluating the pharmacology of sustained changes in $[Ca^{2+}]_i$ at WT fluo-3-loaded vHipp axons. The $\alpha 7^*$ nAChRs-selective antagonist α BgTx (100 nM) eliminated sustained nicotine-induced increase in $[Ca^{2+}]_i$, whereas the ($\alpha\beta$)*nAChR antagonist DH β E (1 μ M) did not. 5-Iodo-A-85380 (10 μ M), a non- $\alpha 7^*$ nAChRs agonist, did not elicit a sustained increase in $[Ca^{2+}]_i$. ** $p < 0.01$; ANOVA, Holm–Sidak test.

whether the ventral hippocampal slice was derived from WT or from *Nrg1^{tm1Lwr} +/-* mice (see Figs. 1G, 2, 3). Glutamatergic miniature postsynaptic currents (Glu mEPSCs) were recorded in the presence of bicuculline (20 μ M) and TTX (2 μ M), and Glu mEPSCs were blocked by application of CNQX (10 μ M) and APV (50 μ M).

Sustained enhancement of hippocampal–accumbens glutamatergic transmission by nicotine

Continuous recording of glutamatergic transmission at +/+ to +/+ synapses during and after a brief exposure to a low concentration of nicotine (1 min, 100–500 nM) revealed a sustained

(>30 min) enhancement of transmission (Fig. 2). The frequency of Glu mEPSCs increased 2.8 ± 0.3 -fold (from 3–4 to 8–14 Hz; $n = 8$) when nicotine was applied. The initial increase in Glu mEPSC frequency was followed by a sustained, 2.0 ± 0.1 -fold increase above the pre-nicotine Glu mEPSC frequency (Fig. 2A–C). The nicotine-induced enhancement of glutamatergic synaptic transmission was partially blocked by nAChR subtype-selective antagonists and completely blocked by general nicotinic antagonists (e.g., mecamylamine; data not shown). Most notably, pretreatment with the $\alpha 7^*$ nAChRs-selective antagonist α BgTx eliminated the sustained enhancement of glutamatergic transmission but left the transient enhancement of transmission by nicotine intact (Fig. 2B). Brief application of nicotine also resulted in sustained, focal increases in $[Ca^{2+}]_i$ along vHipp axons (Fig. 2D) (supplemental Fig. 1, available at www.jneurosci.org as supplemental material). The sustained, nicotine-induced increases in presynaptic $[Ca^{2+}]_i$ were blocked by α BgTx but not by dihydro- β -erythroidine (DH β E). A non- $\alpha 7^*$ nAChRs agonist (5-Iodo-A-85380) did not elicit a sustained increase in presynaptic $[Ca^{2+}]_i$.

Type III Nrg1 chimeric vHipp → nAcc synapses lack sustained enhancement of glutamatergic transmission

We next examined the effects of nicotine on glutamatergic transmission at synapses between *Nrg1^{tm1Lwr} +/-* vHipp and +/+ nAcc neurons. The magnitude of the rapid nicotine-induced facilitation detected at chimeric synapses was comparable with that detected at +/+ to +/+ synapses (Fig. 3A–C). However, at chimeric synapses, the nicotine-induced synaptic facilitation was short-lived (Fig. 3A–C), returning to control levels immediately after washout of nicotine (Fig. 3B). The nAChR-mediated enhancement of glutamatergic transmission at chimeric synapses was insensitive to the $\alpha 7^*$ nAChRs-selective antagonist α BgTx (Fig. 3B).

The brief nature of the nicotine-induced enhancement of glutamatergic transmission at chimeric synapses was paralleled by a transient, rather than a sustained, increase in presynaptic $[Ca^{2+}]_i$ (Fig. 3D). Pooled data summarizing the effect of presynaptic, monoallelic deletion of type III Nrg1 on the modulation of hippocampal glutamatergic transmission and on presynaptic $[Ca^{2+}]_i$ are presented in Figure 3D and supplemental Figure 2 (available at www.jneurosci.org as supplemental material). In chimeric circuits, the sustained, α BgTx-sensitive component of nicotine-enhanced transmission was abolished, whereas the transient effects on both glutamate release and Ca^{2+} signaling were preserved. These data are consistent with a selective loss of functional $\alpha 7^*$ nAChRs at presynaptic sites

along *Nrg1^{tm1Lwr} +/-* vHipp axonal projections, without loss of non- $\alpha 7^*$ nAChRs that support transient responses to nicotine.

Type III Nrg1 back-signaling increases surface expression of $\alpha 7^*$ nAChRs along vHipp axons

To assess whether the loss of $\alpha 7^*$ nAChRs response at type III Nrg1 chimeric synapses was attributable to decreased axonal $\alpha 7^*$ nAChRs expression, we measured $\alpha 7^*$ nAChRs levels in vHipp explants and along vHipp projections. Analysis of hippocampal axons revealed >70% decrease in the fraction of vGluT⁺ axons that colabeled with α BgTx in *Nrg1^{tm1Lwr} +/-* vHipp to WT nAcc compared with *+/+* vHipp to *+/+* nAcc cocultures (Fig. 4A,B). Total $\alpha 7$ protein levels in vHipp microslices from *Nrg1^{tm1Lwr} +/-* mice were ~40% lower than levels in WT slices (Fig. 4D). These results indicate that WT levels of type III Nrg1 signaling are required for expression of functional presynaptic $\alpha 7^*$ nAChRs.

Type III Nrg1 functions as a bidirectional signaling molecule (Bao et al., 2003; Hancock et al., 2008). To test the possibility that axonal type III Nrg1, acting as a receptor, regulates $\alpha 7^*$ nAChRs levels along axons, we treated vHipp microslices with the extracellular domain of ErbB4 (B4-ECD, 2 nM) for 1, 6, or 24 h. We visualized $\alpha 7^*$ nAChRs present on the surface of vHipp axons by staining live preparations with labeled α BgTx (red) before fixation. When vHipp microslices from *Nrg1^{tm1Lwr} +/-* animals were treated with B4-ECD for 6 or 24 h (but not after 1 h), levels of $\alpha 7^*$ nAChRs clusters at glutamatergic synapses increased from ~12 per 100 μ m to ~40 per 100 μ m axon length, a level comparable with that seen in *+/+* microslices (treatment of *+/+* vHipp microslices with B4-ECD increased the number of $\alpha 7^*$ nAChRs clusters from ~30 clusters/100 μ m to ~40 clusters/100 μ m) (Fig. 4B). Microslices from *Nrg1^{tm1Lwr} -/-* animals did not respond to B4-ECD treatment (supplemental Fig. 3D, available at www.jneurosci.org as supplemental material). To determine whether the B4-ECD-induced increase in $\alpha 7^*$ nAChRs resulted from recruitment of preexisting intracellular pools, we repeated the B4-ECD treatment of *+/+* and *+/-* microslices in the presence of cycloheximide (CHX) for 6 h. CHX treatment alone did not affect levels of α BgTx staining but eliminated the B4-ECD-induced increase in $\alpha 7^*$ nAChRs levels (Fig. 4C). B4-ECD treatment of vHipp microslices from *Nrg1^{tm1Lwr} +/-* animals also restored the ability of these neurons to mount a sustained elevation of intracellular calcium in response to brief exposure to nicotine (Fig. 3D). Thus, increased type III Nrg1 back-signaling in *Nrg1^{tm1Lwr} +/-* vHipp microslices restored functional axonal $\alpha 7^*$ nAChRs to WT levels.

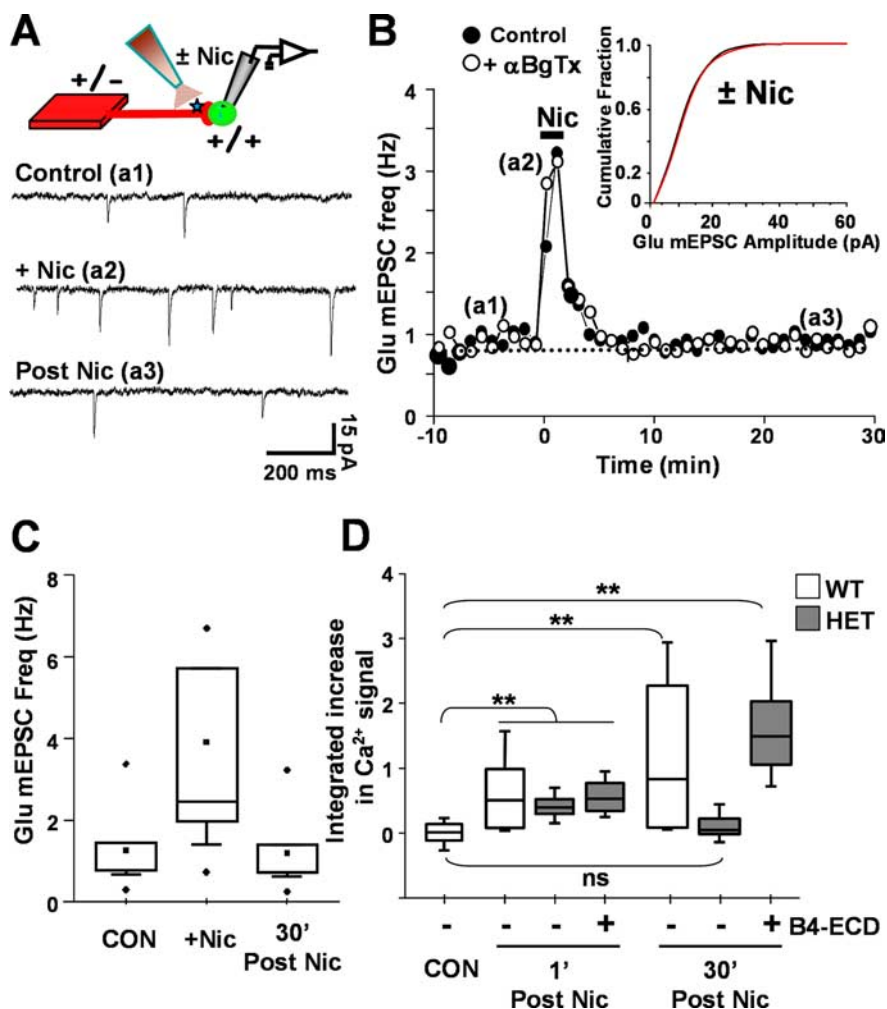


Figure 3. Nicotine enhancement of transmission at *Nrg1^{tm1Lwr} +/-* vHipp to WT nAcc synapses is brief. **A**, Top, Schematic diagram of the recording configuration in assays of glutamatergic synapses in *+/+* vHipp slice (red) and dispersed WT nAcc neurons (green). **a1**, Control Glu mEPSCs (bicuculline and TTX resistant; CNQX-APV sensitive). **a2**, Spontaneous synaptic currents with nicotine (+Nic) recorded in the same nAcc neurons ~2 min after application and washout of nicotine (500 nM; 1 min). **a3**, Postnicotine records obtained ~30 min after a 1 min nicotine application and washout. **B**, In contrast to WT vHipp to WT nAcc transmission, the nicotine-induced enhancement of mEPSC frequency was brief (filled circles) and insensitive to α BgTx (open circles) at *Nrg1^{tm1Lwr} +/-* to WT synapses. Inset in **B**, There was no effect of nicotine on mEPSC amplitude (control, black; +Nic, red) sampled at 5 min before, during, and immediately after nicotine application (**a1**, **a2**, and **a3**, respectively). **C**, Box plot of pooled data ($n = 8$ for each condition) examining the time course of modulation of transmission at *Nrg1^{tm1Lwr} +/-* vHipp to *+/+* nAcc synapses. Although there were significant effects of nicotine on short-term Glu mEPSC frequency (CON vs Nic, $p < 0.01$), the enhancement of synaptic transmission did not persist (CON vs Nic 30 min; not significant). Note that the fold effect of nicotine on increasing glutamate receptor mEPSCs was comparable, but the baseline mEPSC frequency was typically lower and the nicotine response more variable in *Nrg1^{tm1Lwr} +/-* to *+/+* than those recorded in *+/+* to *+/+* cocultures. **D**, Box plot of pooled data ($n = 3$) of nicotine-induced changes in $[Ca^{2+}]_i$ along *+/+* versus *+/-* fluo-3-loaded vHipp axons. The acute effects of nicotine on $[Ca^{2+}]_i$ were comparable for *+/+* versus *+/-* vHipp axons (with or without B4-ECD treatment). In contrast, the sustained increase in calcium signaling seen ≥ 20 min after nicotine treatment at *+/+* vHipp axons was not detected in *Nrg1^{tm1Lwr} +/-* vHipp axons. Incubation with B4-ECD (24 h) rescued this deficit. $**p < 0.01$. HET, Heterozygous animals.

Discussion

Using an *in vitro* microslice preparation that permits examination of CNS synapses comprising genetically distinct presynaptic versus postsynaptic neurons, we demonstrate that type III Nrg1 is required for nicotine-induced sustained potentiation of glutamatergic transmission at hippocampal-accumbens synapses. The persistent phase of glutamatergic facilitation, which lasts up to 1 h after a single, 1 min exposure to 100 nM nicotine, is mediated by presynaptic $\alpha 7^*$ nAChRs. Decreased expression of presynaptic type III Nrg1 results in an ~80% reduction in functional $\alpha 7^*$ nAChRs on axonal surfaces, as assessed by α BgTx staining

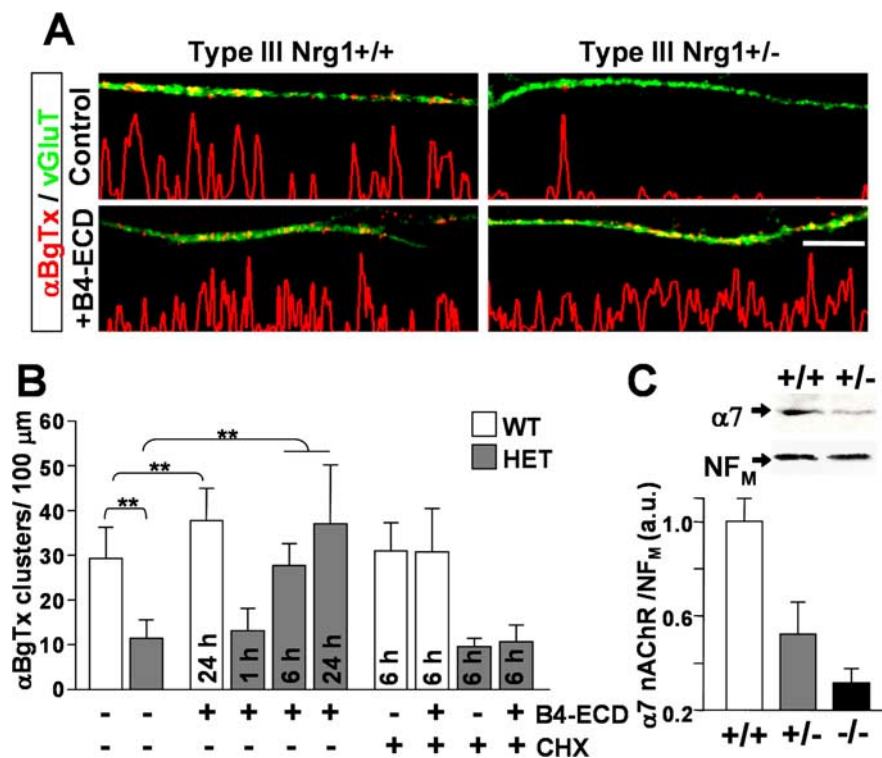


Figure 4. Type III Nrg1 signaling regulates expression of $\alpha 7$ nAChRs along vHipp axons. **A**, vHipp explants from either $+/+$ or $Nrg1^{tm1Lwr} +/-$ mice were labeled for surface $\alpha 7$ nAChRs with α Bgtx–Alexa 594 (red). Cultures were then fixed, permeabilized, and stained with antibodies recognizing vGluT (green). Representative micrographs of WT (left) and $Nrg1^{tm1Lwr} +/-$ (right) vHipp axons are shown above line scans of fluorescence intensity profile for α Bgtx staining. Top, There is a significant decrease in the number of α Bgtx-labeled clusters along axons from $Nrg1^{tm1Lwr} +/-$ explants compared with WT (plotted in **B**). Bottom, After treatment with B4-ECD, the number of α Bgtx-labeled clusters increased along both WT and $Nrg1^{tm1Lwr} +/-$ axons. Magnification, $40\times$. Scale bar, $5\ \mu\text{m}$. **B**, α Bgtx clusters along axons were quantified under control or after 1, 6, or 24 h B4-ECD treatment. The level of surface α Bgtx clusters was lower on $Nrg1^{tm1Lwr} +/-$ versus $+/+$ axons (11.6 ± 3.9 vs 29.5 ± 7 clusters/100 μm). A 24 h B4-ECD treatment induced a 1.3-fold increase in surface α Bgtx clusters along WT vGluT $^+$ axons: control, 29.5 ± 7.0 versus B4-ECD, 38.1 ± 7.2 clusters/100 μm axon. B4-ECD treatment for 6 or 24, but not 1 h, increased surface α Bgtx staining along $Nrg1^{tm1Lwr} +/-$ axons: control, 11.6 ± 3.9 versus 1 h B4-ECD, 13.1 ± 6.6 ; 6 h B4-ECD, 28.8 ± 6.2 ; and 24 h B4-ECD, 37.5 ± 12.9 clusters/100 μm axon. In parallel, vHipp microslices were treated with $10\ \mu\text{M}$ CHX with and without B4-ECD for 6 h. CHX blocked the B4-ECD-induced increase in α Bgtx binding in both $+/+$ and $+/-$ cultures. $***p < 0.01$. **C**, Total ventral hippocampal $\alpha 7$ protein was measured by immunoblotting. $Nrg1^{tm1Lwr} +/-$ vHipp lysate had an $\sim 40\%$ reduction in total $\alpha 7$ protein compared with WT. HET, Heterozygous animals.

and nicotine-elicited changes in axonal $[\text{Ca}]_i$. Incubation of vHipp microslices with recombinant B4-ECD increased the levels of surface $\alpha 7$ nAChRs along glutamatergic projections from WT vHipp microslices and restored levels of surface $\alpha 7$ nAChRs along glutamatergic projections from $+/-$ vHipp microslices. Whether the increase in surface $\alpha 7$ nAChRs reflects a specific effect of ErbB4/Nrg1 signaling on the $\alpha 7$ subunit per se or is secondary to more general response of $\alpha 7$ nAChRs-expressing vHipp projection neurons is not clear at this time. We propose that presynaptic type III Nrg1 is required for the normal levels of expression and axonal targeting of $\alpha 7$ nAChRs.

Expression and somatodendritic trafficking of $\alpha 7$ nAChRs is regulated by Nrg1/ErbB and neurotrophin/Trk signaling (Yang et al., 1998; Liu et al., 2001; Kawai et al., 2002; Chang and Fischbach, 2006; Massey et al., 2006; Hancock et al., 2008). Our current results are distinct from previous studies in that the requirement for type III Nrg1 is cell autonomous, i.e., presynaptic type III Nrg1 regulates presynaptic $\alpha 7$ nAChRs. Type III Nrg1 isoforms have the capacity to participate in bidirectional, juxtacrine signaling that involves both transcriptional responses and local signaling in axons (Bao et al., 2003; Hancock et al., 2008). We propose

that the $\alpha 7$ nAChRs is a target of both forward signaling downstream of activated ErbB receptors and reverse signaling. Within the hippocampus, Nrg1/ErbB signaling regulates levels of $\alpha 7$ nAChRs on interneurons (Liu et al., 2001; Chang and Fischbach, 2006). We now demonstrate that type III Nrg1 reverse signaling regulates $\alpha 7$ nAChRs expression and targeting to ventral hippocampal axonal projections. In this manner, Nrg1/ErbB signaling affects cholinergic modulation within hippocampal circuits as well as cholinergic modulation of hippocampal output.

The chimeric *in vitro* preparation from $Nrg1^{tm1Lwr}$ mice described here provides an informative approach for studying the role of Nrg1 signaling in both presynaptic and postsynaptic mechanisms of synaptic plasticity. The modulatory influence of ACh on ventral striatal circuits involves both muscarinic and nicotinic receptors, as well as presynaptic and postsynaptic mechanisms (Ge and Dani, 2005; Wang et al., 2006). Current findings support the proposal that genetic modifications of Nrg1-mediated signaling in presynaptic inputs changes the presynaptic profile of nAChRs and thereby alters the temporal profile of responses to nicotine. Alterations in this temporal profile might lead to deficits in sensory gating by altering glutamatergic transmission in corticostriatal circuits (supplemental Fig. 4, available at www.jneurosci.org as supplemental material). In particular, glutamatergic transmission from vHipp to nAcc is thought to be involved in the regulation of sensory gating or prepulse inhibition (PPI), and PPI deficits are a common endophenotype of schizophrenia. Self-administration of nicotine might represent a means of coping

with the altered temporal response to nicotine and might underlie the ameliorating effect of nicotine administration on PPI deficits as proposed previously (Bast and Feldon, 2003; Zoranzo et al., 2005).

References

- Bao J, Wolpowitz D, Role LW, Talmage DA (2003) Back signaling by the Nrg-1 intracellular domain. *J Cell Biol* 161:1133–1141.
- Bast T, Feldon J (2003) Hippocampal modulation of sensorimotor processes. *Prog Neurobiol* 70:319–345.
- Batel P (2000) Addiction and schizophrenia. *Eur Psychiatry* 15:115–122.
- Bjarnadottir M, Misner DL, Haverfield-Gross S, Bruun S, Helgason VG, Stefansson H, Sigmundsson A, Firth DR, Nielsen B, Stefansson R, Novak TJ, Stefansson K, Gurney ME, Andresson T (2007) Neuregulin1 (NRG1) signaling through Fyn modulates NMDA receptor phosphorylation: differential synaptic function in NRG1 $^{+/-}$ knock-outs compared with wild-type mice. *J Neurosci* 27:4519–4529.
- Chang Q, Fischbach GD (2006) An acute effect of neuregulin 1 β to suppress $\alpha 7$ -containing nicotinic acetylcholine receptors in hippocampal interneurons. *J Neurosci* 26:11295–11303.
- Couey JJ, Meredith RM, Spijker S, Poorthuis RB, Smit AB, Brussaard AB, Mansvelter HD (2007) Distributed network actions by nicotine in-

- crease the threshold for spike-timing-dependent plasticity in prefrontal cortex. *Neuron* 54:73–87.
- Dajas-Bailador F, Wonnacott S (2004) Nicotinic acetylcholine receptors and the regulation of neuronal signalling. *Trends Pharmacol Sci* 25:317–324.
- Falls DL (2003) Neuregulins: functions, forms, and signaling strategies. *Exp Cell Res* 284:14–30.
- Ge S, Dani JA (2005) Nicotinic acetylcholine receptors at glutamate synapses facilitate long-term depression or potentiation. *J Neurosci* 25:6084–6091.
- Gu Z, Jiang Q, Fu AK, Ip NY, Yan Z (2005) Regulation of NMDA receptors by neuregulin signaling in prefrontal cortex. *J Neurosci* 25:4974–4984.
- Hancock ML, Canetta SE, Role LW, Talmage DA (2008) Presynaptic type III neuregulin1-ErbB signaling targets $\alpha 7$ nicotinic acetylcholine receptors to axons. *J Cell Biol* 181:511–521.
- Harrison PJ, Weinberger DR (2005) Schizophrenia genes, gene expression, and neuropathology: on the matter of their convergence. *Mol Psychiatry* 10:40–68; image 5.
- Huang YZ, Won S, Ali DW, Wang Q, Tanowitz M, Du QS, Pelkey KA, Yang DJ, Xiong WC, Salter MW, Mei L (2000) Regulation of neuregulin signaling by PSD-95 interacting with ErbB4 at CNS synapses. *Neuron* 26:443–455.
- Jo YH, Wiedl D, Role LW (2005) Cholinergic modulation of appetite-related synapses in mouse lateral hypothalamic slice. *J Neurosci* 25:11133–11144.
- Kawai H, Zago W, Berg DK (2002) Nicotinic $\alpha 7$ receptor clusters on hippocampal GABAergic neurons: regulation by synaptic activity and neurotrophins. *J Neurosci* 22:7903–7912.
- Kumari V, Postma P (2005) Nicotine use in schizophrenia: the self medication hypotheses. *Neurosci Biobehav Rev* 29:1021–1034.
- Kwon OB, Longart M, Vullhorst D, Hoffman DA, Buonanno A (2005) Neuregulin-1 reverses long-term potentiation at CA1 hippocampal synapses. *J Neurosci* 25:9378–9383.
- Leonard S, Gault J, Adams C, Breese CR, Rollins Y, Adler LE, Olincy A, Freedman R (1998) Nicotinic receptors, smoking and schizophrenia. *Restor Neurol Neurosci* 12:195–201.
- Li B, Woo RS, Mei L, Malinow R (2007) The neuregulin-1 receptor erbB4 controls glutamatergic synapse maturation and plasticity. *Neuron* 54:583–597.
- Lisman JE, Grace AA (2005) The hippocampal-VTA loop: controlling the entry of information into long-term memory. *Neuron* 46:703–713.
- Liu Y, Ford B, Mann MA, Fischbach GD (2001) Neuregulins increase $\alpha 7$ nicotinic acetylcholine receptors and enhance excitatory synaptic transmission in GABAergic interneurons of the hippocampus. *J Neurosci* 21:5660–5669.
- Mansvelter HD, van Aerde KI, Couey JJ, Brussaard AB (2006) Nicotinic modulation of neuronal networks: from receptors to cognition. *Psychopharmacology (Berl)* 184:292–305.
- Massey KA, Zago WM, Berg DK (2006) BDNF up-regulates $\alpha 7$ nicotinic acetylcholine receptor levels on subpopulations of hippocampal interneurons. *Mol Cell Neurosci* 33:381–388.
- Mathew SV, Law AJ, Lipska BK, Davila-Garcia MI, Zamora ED, Mitkus SN, Vakkalanka R, Straub RE, Weinberger DR, Kleinman JE, Hyde TM (2007) $\alpha 7$ nicotinic acetylcholine receptor mRNA expression and binding in postmortem human brain are associated with genetic variation in neuregulin 1. *Hum Mol Genet* 16:2921–2932.
- McGehee DS, Heath MJ, Gelber S, Devay P, Role LW (1995) Nicotine enhancement of fast excitatory synaptic transmission in CNS by presynaptic receptors. *Science* 269:1692–1696.
- Okada M, Corfas G (2004) Neuregulin1 downregulates postsynaptic GABAA receptors at the hippocampal inhibitory synapse. *Hippocampus* 14:337–344.
- Ronesi J, Lovinger DM (2005) Induction of striatal long-term synaptic depression by moderate frequency activation of cortical afferents in rat. *J Physiol (Lond)* 562:245–256.
- Stefansson H, Steinthorsdottir V, Thorgeirsson TE, Gulcher JR, Stefansson K (2004) Neuregulin 1 and schizophrenia. *Ann Med* 36:62–71.
- Strand JE, Nybäck H (2005) Tobacco use in schizophrenia: a study of cotinine concentrations in the saliva of patients and controls. *Eur Psychiatry* 20:50–54.
- Wang Z, Kai L, Day M, Ronesi J, Yin HH, Ding J, Tkatch T, Lovinger DM, Surmeier DJ (2006) Dopaminergic control of corticostriatal long-term synaptic depression in medium spiny neurons is mediated by cholinergic interneurons. *Neuron* 50:443–452.
- Wolpowitz D, Mason TB, Dietrich P, Mendelsohn M, Talmage DA, Role LW (2000) Cysteine-rich domain isoforms of the neuregulin-1 gene are required for maintenance of peripheral synapses. *Neuron* 25:79–91.
- Yang X, Kuo Y, Devay P, Yu C, Role L (1998) A cysteine-rich isoform of neuregulin controls the level of expression of neuronal nicotinic receptor channels during synaptogenesis. *Neuron* 20:255–270.
- Zornoza T, Cano-Cebrián MJ, Miquel M, Aragón C, Polache A, Granero L (2005) Hippocampal dopamine receptors modulate the motor activation and the increase in dopamine levels in the rat nucleus accumbens evoked by chemical stimulation of the ventral hippocampus. *Neuropsychopharmacology* 30:843–852.